The International Journal of Advanced Manufacturing Technology (2020) 106:5345–5352
https://doi.org/10.1007/s00170-020-04993-9

ORIGINAL ARTICLE

Effects of hole diameter and ply angle on the mechanical behaviour of hole-clinched joints in carbon fibre reinforced polymers and aluminium alloy sheets

Yang Liu[1] · Weimin Zhuang[1] · Shijie Wu[2]

Received: 31 May 2019 / Accepted: 27 January 2020 / Published online: 6 February 2020
© Springer-Verlag London Ltd., part of Springer Nature 2020

Abstract
The present paper investigates the joinability of unidirectional carbon fibre reinforced polymers (CFRP) and aluminium alloys by the method of hole clinching. The static properties and failure process of the single-lap joints were tested. The effects of the hole diameter and the ply angle of CFRP on the static properties and failure processes of hole-clinched joints are discussed. The obtained results demonstrated that the joints with different ply angles have similar maximum loads, while the ply angle affects the failure mode of the joints. Increasing the hole diameter of the CFRP enhances the strength and energy absorption of the joints.

Keywords Hole clinching · CFRP · Failure process · Static properties · Hole diameter · Ply angle

1 Introduction

Owing to the pressure imposed by energy shortages and environmental pollution, the structure lightweight has become the main trend of industrial manufacturing [1–3]. Carbon fibre reinforced polymers (CFRP) have been widely applied in the automotive and aerospace industries due to their remarkable characteristics, such as a high strength-to-density ratio, superior fatigue performance and excellent corrosion resistance [4–6].

The application of multi-material structures poses challenges to joining techniques [7]. Some emerging joining technologies that can solve the problems of the traditional joining process have appeared, such as clinching [8–11], self-piercing riveting [12–15], bonding [16], and friction stir welding [17–19]. Each joining technology has unique advantages and can be applied in appropriate conditions. Mechanical clinching is a simple and cheap joining method that requires no additional part, such as a rivet or bolt, during the joining process, and the clinched joints have superior fatigue performance [20].

✉ Weimin Zhuang
zhuangwm@jlu.edu.cn

[1] State Key Laboratory of Automotive Simulation and Control, Jilin University, Changchun 130022, China

[2] SAIC Volkswagen Automotive Co. Ltd., Shanghai 201800, China

However, an inherent drawback of clinching appears in joining low ductility materials, such as magnesium alloy and fibre reinforced polymers. When joining the composite sheet, damage induced in the joining process should be considered comprehensively. Cracking is inevitable in the composite materials due to the large localized deformation that sheet materials undergo during the joining process. The forming damage of composite sheet affects the appearance and mechanical properties of the joint [15]. Lee et al. [21] proposed a clinching method for pre-punching the lower composite sheet. The metallic material with better ductility was used as the upper sheet, and the punch expanded the upper sheet in the lower sheet hole to form an interlock structure. Hole clinching is a mechanical cold-forming technique that has been considered an economical and effective process to join composite sheets in many industrial fields. The process of hole clinching is shown in Fig. 1. Lee et al. [22] used numerical simulation and experimental methods to identify the hole clinching process, and discussed the effect of punch shape on the interlocking parameters and static strength of hole-clinched joints. It found that using the punch with sharp corner resulted in the neck thickness decreased and tended to cause neck fracture. Lee et al. [23] optimized the forming quality of hole-clinched joint by using a spring die, which improved the formability of the aluminium alloy and reduced the damage to CFRP. Lambiase et al. [24] invented friction-assisted clinching to cope with the cracking problem in joining low ductility materials and reduce the joining force. Experiments showed that

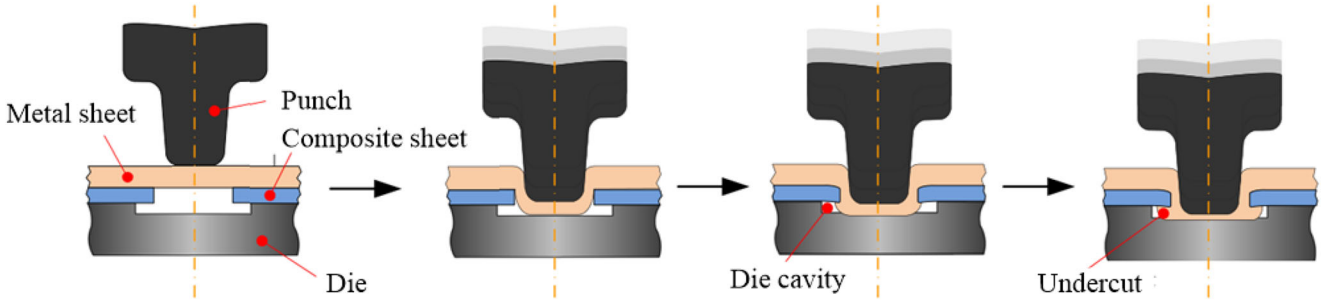

Fig. 1 The process of hole clinching [23]

the joint was obtained with good forming quality, even with the use of sharp tools. The relationship between interlocking parameters and failure modes of the hole-clinched joint under pull-out loading conditions was analysed by Lee et al. [25]. As reviewed above, previous studies published regarding hole clinching of CFRP focused on the composite sheets with braided tissue. Thus, almost no relevant researches have been done for the comprehensive comparison between the hole-clinched joints of CFRP with different ply angles and hole diameters.

At present, single-lap hole-clinched joints in CFRP and AA5754 aluminium alloy were prepared. A comparative investigation focused on the failure modes, failure processes, and static properties between the joints with different ply angles and hole diameters were conducted.

2 Experimental details

2.1 Materials

The obtained joints were fabricated with the CFRP and AA5754 sheets. The CFRP were made of epoxy resin and T300 unidirectional fibre fabrics. The AA5754 sheets were sheared along the rolling direction to 95 mm × 35 mm × 1.5 mm. The mechanical properties of the used materials are listed in Tables 1 and 2, respectively. The design of the hole diameters and the sheet thicknesses of CFRP are based on the reference [23]. The CFRP sheet was sized 95 mm × 35 mm × 1 mm, the hole diameters (D_H) in the CFRP were 8 mm, 8.2 mm, and 8.4 mm, and the lamination sequences of the CFRP were $[45°/-45°]_3$, $[0°/90°]_3$, and [45°/90°/− 45°/0°/90°/45°], respectively.

2.2 Specimen preparation

The servo-hydraulic clinching machine produced by Wuhan Jiarui Riveting Company in China was used to joining the sheets. The overlapping area is 35 mm × 35 mm. The joining process was controlled by the punch displacement to achieve a bottom thickness of 0.4 mm in each joint, and the punch velocity of 1 mm/s was applied. The geometries of the punch and die are shown in Fig. 2. For simplicity, the different hole-clinched joints are denoted in Table 3.

The forming quality was evaluated using the cross-section visual inspection method based on the geometrical parameters of the neck thickness (T_N), undercut (T_U), and bottom thickness (X), as shown in Fig. 3. The typical cross-sections of joints are presented in Fig. 4; each joint forms an effective interlocking structure. Figure 5 depicts the changes of neck

Table 1 Material properties of the CFRP

Property	Symbol	Value
Density (kg/m^3)	ρ	1530
Longitudinal Young's modulus (GPa)	E_{11}	127
Transverse Young's modulus (GPa)	E_{22}	8.41
Young's modulus in the thickness direction (GPa)	E_{33}	8.41
Shear modulus (GPa)	G_{12}, G_{23}, G_{13}	4.41
Poisson's ratio	ν_{12}	0.31
Longitudinal tensile strength (MPa)	X_t	2097
Longitudinal compressive strength (MPa)	X_c	1258
Transverse tensile strength (MPa)	Y_t	42
Transverse compressive strength (MPa)	Y_c	175
Tensile strength in the thickness direction (MPa)	Z_t	42
Compressive strength in the thickness direction (MPa)	Z_c	175
Shear strength (MPa)	S_{12}, S_{23}, S_{13}	90

Table 2 Mechanical properties of the AA5754 sheet

Density (kg/m^3)	Elastic modulus (GPa)	Tensile strength (MPa)	Yield strength (MPa)	Poisson's ratio
2700	70	244.1	162.1	0.3

thickness and undercut with the hole diameter. The increase of hole diameter results in the increase of neck thickness and the decrease of undercut value. An increased punch-hole clearance resulted in more material remaining in the neck, which led to the decrease of material flow in the upsetting stage and the smaller undercut in the joints.

2.3 Tensile-shear tests

Tensile-shear tests were carried out using a WDW3100 universal testing machine produced by Jilin Guanteng Automation Technology Co., Ltd., China. Two spacers with corresponding thicknesses were attached on the two ends of the specimens to eliminate additional bending. A tensile speed of 2 mm/min was adopted, and five specimens were repeatedly tested in each condition.

3 Results and discussion

3.1 Failure mode

As shown in Fig. 6, the failed joints reveal three types of failure modes: neck fracture, hybrid neck fracture, and button separation. The hybrid neck fracture is composed of interlock failure and neck fracture because the strength of the interlock is slightly larger than that of the joint neck. This failure mode occurred in the B8.2 joint and the A8.4 joint, and the bottom button in the B8.2 joint deformed severely. Delamination in the bearing region around the hole, fibre fracture, and matrix cracks along the fibre directions were presented in the failure mode of the button separation. Delamination in the B8.4 joint arose throughout the CFRP thickness, which was attributed to the presence of more 0° layers in the $[0°/90°]_3$ CFRP, which was liable for introducing matrix cracking parallel to the loading direction. It could be concluded that button separation usually occurred in the hole-clinched joint with a complex ply angle; delamination only occurred between the layers in the compression region of the CFRP, and the matrix damage in the upper surface was the most severe.

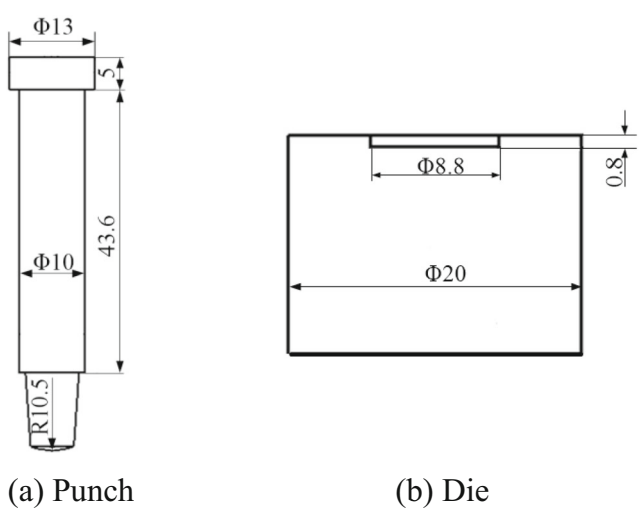

Fig. 2 Geometries of the punch and die (dimensions in mm). **a** Punch. **b** Die

3.2 Failure process

The joints with a hole diameter of 8.2 mm present three typical failure modes, and the damage of the CFRP in the B8.4 joint is different from that of the other joints. The above four joints were selected to analyse the failure process. The charge-coupled device (CCD) camera was used to record images in the jointed regions during the tensile tests and the schematic diagram is shown in Fig. 7.

The deformation of the jointed region during the tensile process is shown in Fig. 8, where S represents the total displacement. The failure mode of the A8.2 joint is neck fracture. During the tensile process, the compressive region of the neck was sheared by the wall of the CFRP hole, and the crack propagated towards the non-loading direction. From Fig. 8a, it can be inferred that when the displacement was greater than 0.6S, the upper area of the clinched button was slightly deformed due to the tensile force, and no damage was present on the surface of the CFRP during the tensile process. The failure mode of the B8.2 joint is a hybrid neck fracture. At a displacement of 0.4S, the upper side of the clinched button was bent and deformed, and the matrix cracks along the 0° fibre direction occurred under the circular hole due to the compression of

Table 3 Nomenclature of the different hole-clinched joints

Joint	D_H (mm)	Lamination sequence of CFRP
A8	8	$[45°/-45°]_3$
B8	8	$[0°/90°]_3$
C8	8	[45°/90°/− 45°/0°/90°/45°]
A8.2	8.2	$[45°/-45°]_3$
B8.2	8.2	$[0°/90°]_3$
C8.2	8.2	[45°/90°/− 45°/0°/90°/45°]
A8.4	8.4	$[45°/-45°]_3$
B8.4	8.4	$[0°/90°]_3$
C8.4	8.4	[45°/90°/− 45°/0°/90°/45°]

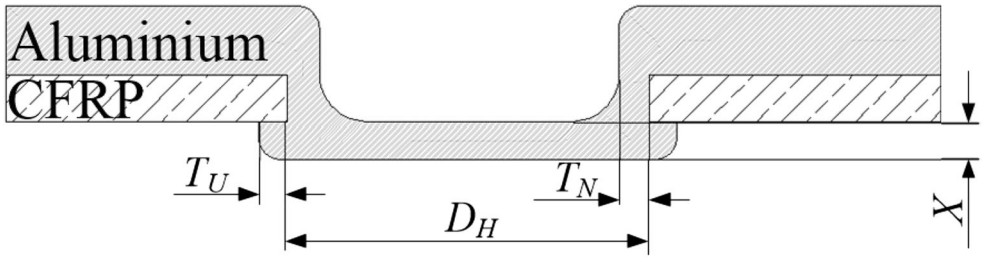

Fig. 3 Quality assessment criteria for the hole-clinched joint

the clinched button; at the same time, the neck of the joint fractured. As the displacement increased further, the crack in the neck continued to propagate, and the upper side of the clinched button bent along the loading direction. At the end of the tensile process, the neck of the joint was completely fractured, and partial interlock structure failure occurred. The failure of the C8.2 joint was due to damage to the CFRP, which resulted in the breakage of the interlock structure. At a displacement of 0.4*S*, matrix cracking, fibre fracture, and delamination occurred in the compression area around the circular hole. From Fig. 8c, matrix cracks along the 45° fibre direction are present on the surface of CFRP. With the increase in displacement, the fibre breakage occurred near the hole, resulting in an increase in the hole diameter, and the clinched button gradually peeled off from the hole. The B8.4 joint failed due to the clinched button separating from the CFRP sheet, but the damage morphology of the CFRP was different from that of the other joints. Similar to the B8.2 joint, matrix cracks appeared on the surface of the CFRP at a displacement of 0.4*S*, while the damage degree in the B8.4 joint was more severe. The neck thickness of the B8.4 joint was 14.6% larger than that of the B8.2 joint, which resulted in a stronger shear resistance of the neck in the B8.4 joint. As the displacement increased to 0.6*S*, the compressed area of the CFRP on the lower side of the clinched button was deformed along the axial direction, resulting in an enlarged hole diameter. At the same time, the CFRP layer in the jointed region warped, and severe delamination occurred in the compression area. With increasing displacement, the warping degree became larger, and the hole diameter gradually expanded. At a displacement of 0.8*S*, the clinched button tended to peel away from the hole, and finally, the interlock structure completely failed.

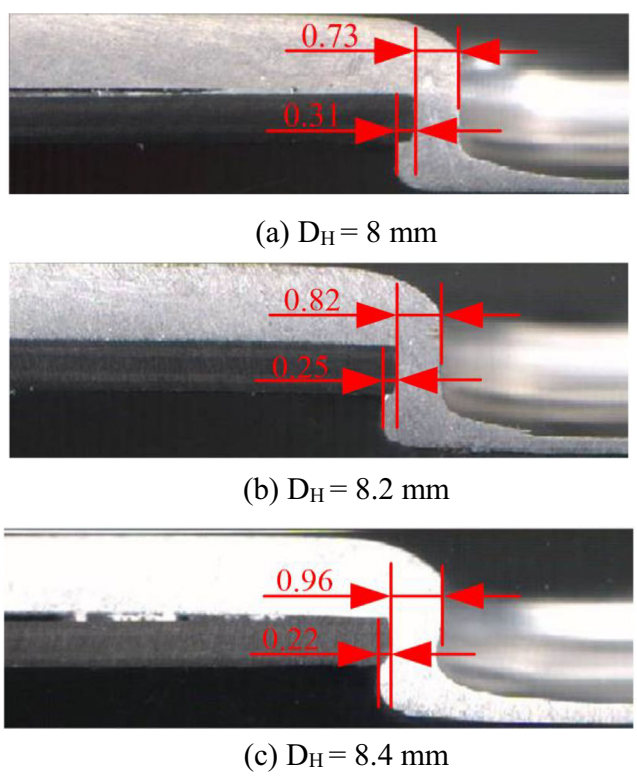

Fig. 4 Cross-section profiles of the joints with different hole diameters (dimensions in mm). **a** $D_H = 8$ mm. **b** $D_H = 8.2$ mm. **c** $D_H = 8.4$ mm

3.3 Static properties

Figure 9 compares the maximum load and energy absorption of different joints. The maximum load of each joint was between 2000 N and 3000 N, and the C8.4 joint obtained the highest peak load of 2906 N. The B8 joint had the lowest peak load of 2187 N, while the C8 joint showed the lowest energy absorption at 2.3 J.

The typical load-displacement curves of the joints with different ply angles are shown in Fig. 10. For the joints with a hole diameter of 8 mm, the curves of the A8 and B8 joints were similar, and the values decreased to approximately 1780 N at the peak loads and then decreased slowly

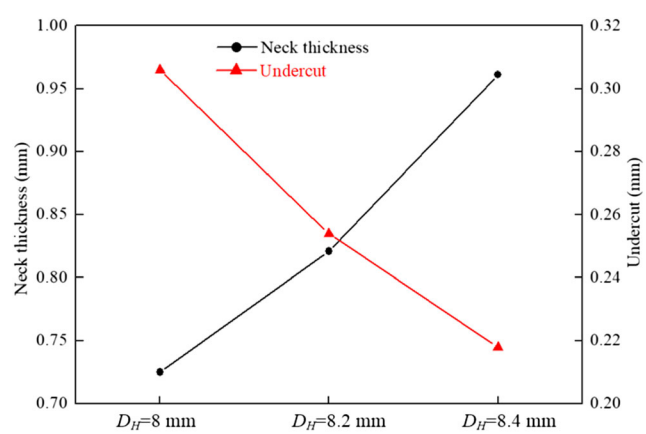

Fig. 5 Variation in the neck thickness and undercut for different hole diameters

until the neck fractured. This was because the A8 and B8 joints had the same failure mechanism, and the crack initiated at a small part of the neck region and expanded progressively along the circumference. The peak load of the C8 joint decreased sharply due to the clinched button that peeled away from the CFRP.

For the joints with a hole diameter of 8.2 mm, the load of the A8.2 joint decreased sharply from 2885 to 1038 N at point A. In the A8.2 joint, a large part of the neck fractured at point A resulting in the load decreased in a large degree, and the joint strength was maintained by the remaining neck structure, and the joint failed quickly. Before point B, the load-displacement curve of the B8.2 joint was similar to that of the B8 joints, while the B8.2 joint had the largest displacement among all the joints. After point B, the load was absorbed by the deformation of the clinched button and was then almost maintained at a constant level. The overall trends of the curves of the C8.2 joint and C8 joint were similar because these joints had the same failure mechanisms.

For joints with a hole diameter of 8.4 mm, the A8.4 joint and C8.4 joint showed different failure modes, but the joints presented the same trend in load-displacement curves. As the load of the A8.4 joint increased to point C, one side of the clinched button started to peel from the pilot hole in the CFRP and the load decreased from 2890 to 2037 N. Subsequently, the joint neck fractured smoothly, resulting in the hybrid neck fracture occurring in the A8.4 joint. For the C8.4 joint, one side of the interlock failed during the initial stretching, and the A8.4 joint and C8.4 joint had almost the same maximum loads due to the same undercut value in both joints. After this, the interlock in the bearing region started to fail by breaking the CFRP layers near the hole. The load-displacement curve of the B8.4 joint was obviously different from those of the joints with a button separation failure mode. After the peak load, the load decreased slowly until the joints completely failed. Before the interlock structure failed, severe damage occurred in the bearing region of the CFRP, the CFRP layers bent, and the hole diameter enlarged, resulting in a smooth decrease in the load. When the CFRP layers deformed to a certain degree, the clinched button gradually pulled out of the hole by breaking the fibres.

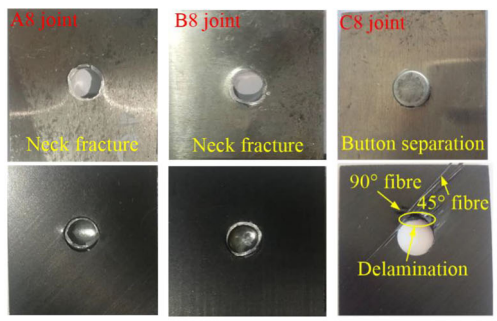

(a) Joints with a hole diameter of 8 mm

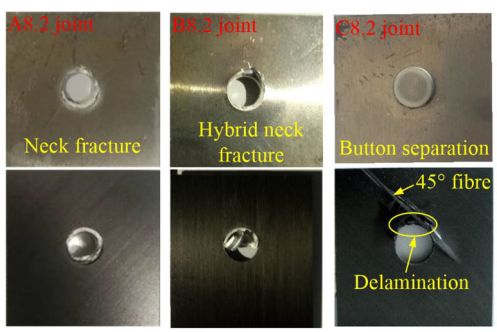

(b) Joints with a hole diameter of 8.2 mm

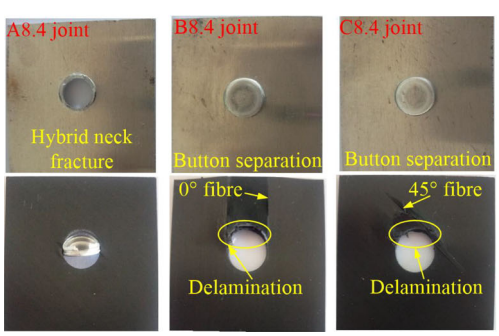

(c) Joints with a hole diameter of 8.4 mm

Fig. 6 Failure modes of the different joints. **a** Joints with a hole diameter of 8 mm. **b** Joints with a hole diameter of 8.2 mm. **c** Joints with a hole diameter of 8.4 mm

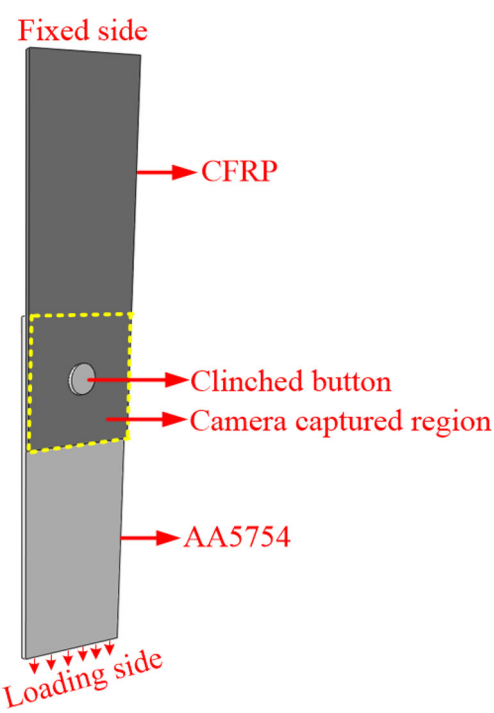

Fig. 7 Schematic diagram of the specimen in the tensile tests

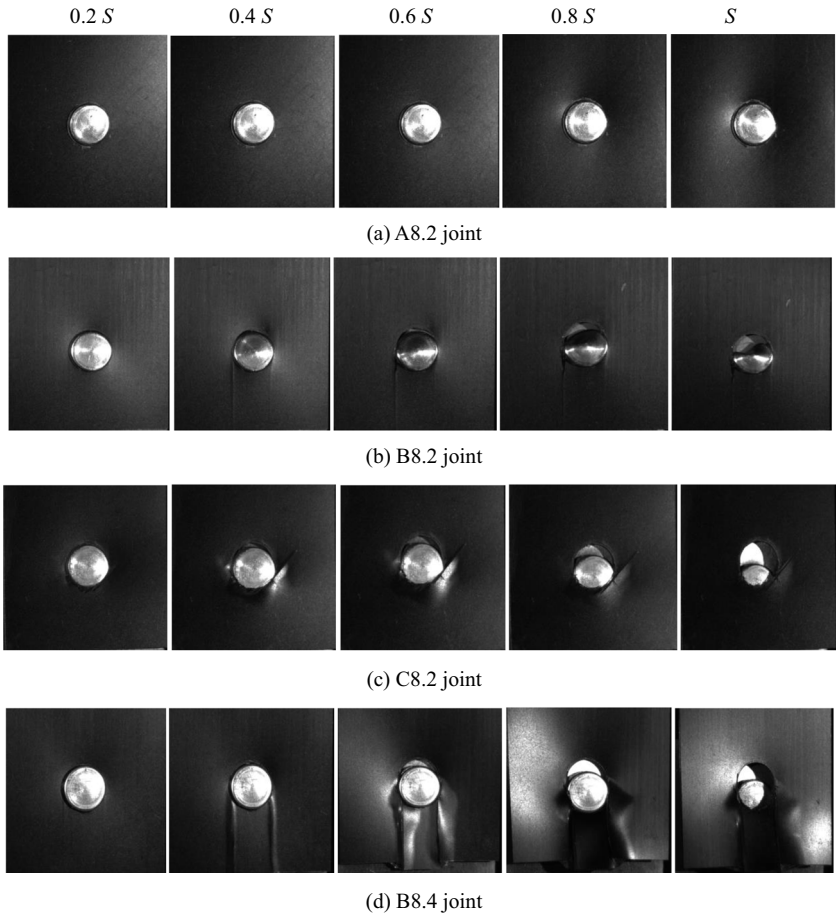

Fig. 8 The deformation of the jointed region during the tensile process. **a** A8.2 joint. **b** B8.2 joint. **c** C8.2 joint. **d** B8.4 joint

3.4 Effect of the ply angle

When the CFRP had the same hole diameter, the joints with different ply angles had a similar maximum load, which was attributed to the strength of the joint being influenced by the neck thickness and undercut. The strength of the joints with $[0°/90°]_3$ CFRP was slightly lower than that of the joints with other ply angles, while the joints with $[0°/90°]_3$ CFRP could obtain the largest displacement. Thus, the joints with $[0°/90°]_3$ CFRP could achieve the optimal property of energy absorption. The ply angle of the CFRP affected the failure mode of the joints; neck fracture was liable to occur in the joints with $[45°/-45°]_3$ CFRP, while the joints with [45°/90°/− 45°/0°/90°/45°] CFRP failed due to button separation.

3.5 Effect of the hole diameter

The typical load-displacement curves of the joints with different hole diameters are shown in Fig. 11. With increasing hole diameter of the CFRP, the maximum loads and energy absorption values of the joints increased, which indicated that the mechanical properties of the joint were mainly affected by the neck thickness. When the ply angles of the lower CFRP sheets were the same, the joints with hole diameters of 8.2 mm and 8.4 mm had similar strengths. As the hole diameter decreased to 8 mm, the maximum load of the joints decreased from 17.7 to 23.4%. The hole diameter influenced the failure mode of the joint with $[0°/90°]_3$ CFRP; with increasing hole diameter in the CFRP, the failure mode of the joint changed from neck fracture to button separation.

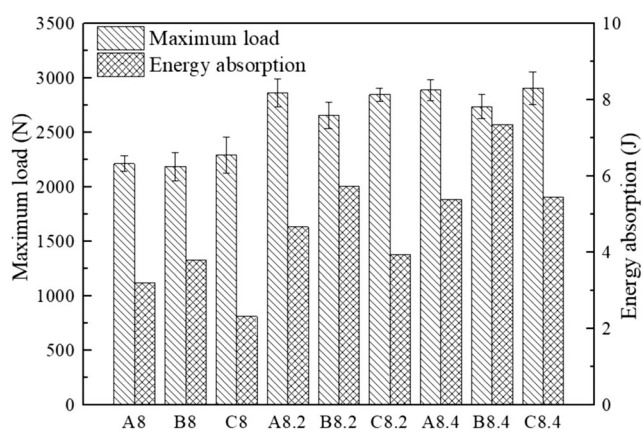

Fig. 9 Average maximum loads and energy absorptions for different joints

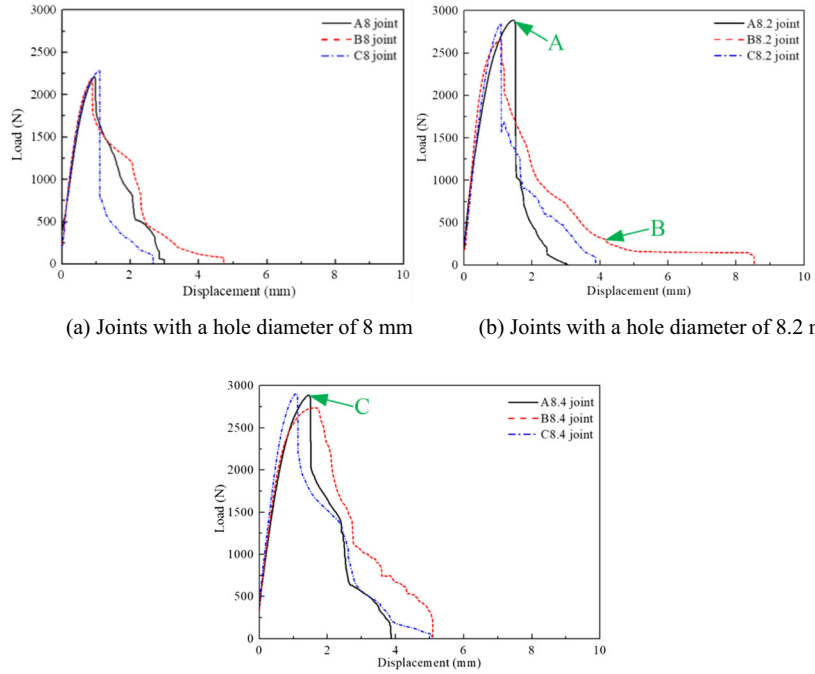

(a) Joints with a hole diameter of 8 mm

(b) Joints with a hole diameter of 8.2 mm

(c) Joints with a hole diameter of 8.4 mm

Fig. 10 Load-displacement curves of the joints with different ply angles. **a** Joints with a hole diameter of 8 mm. **b** Joints with a hole diameter of 8.2 mm. **c** Joints with a hole diameter of 8.4 mm

4 Conclusions

In this study, the static properties and failure processes of hole-clinched joints with different hole diameters and ply angles were investigated. The major conclusions can be drawn as follows:

1. Hole clinching can be applied to join unidirectional CFRP with different ply angles with aluminium alloy sheets. The interlocking structures are formed in the joints, and no obvious damage to the CFRP can be observed.
2. When the CFRP sheets have the same hole diameter, the joints with different ply angles have similar maximum

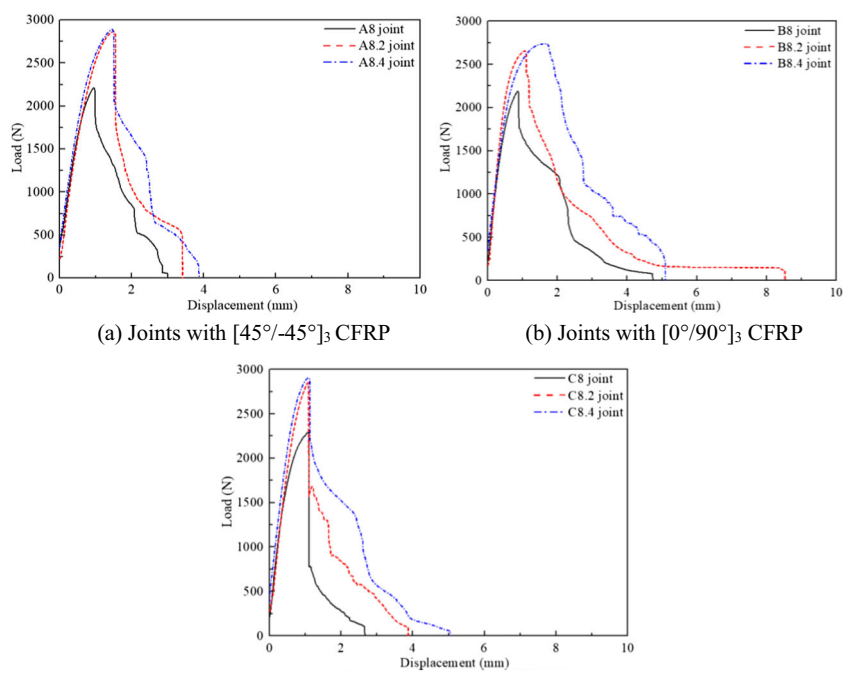

(a) Joints with $[45°/-45°]_3$ CFRP

(b) Joints with $[0°/90°]_3$ CFRP

(c) Joints with [45°/90°/-45°/0°/90°/45°] CFRP

Fig. 11 Load-displacement curves for the joints with different hole diameters. **a** Joints with $[45°/-45°]_3$ CFRP. **b** Joints with $[0°/90°]_3$ CFRP. **c** Joints with [45°/90°/− 45°/0°/90°/45°] CFRP

loads, while the ply angle affects the failure modes of the joints.

3. Neck fracture is likely to occur in the joints with [45°/−45°]$_3$ CFRP, while the failure mode of the joints with [45°/90°/− 45°/0°/90°/45°] CFRP is button separation.
4. Increasing the hole diameter in the CFRP enhances the strength and energy absorption of hole-clinched joints.

Funding information This study is supported by the National Natural Science Foundation of China (Grant nos. 51775227 and 51375201).

References

1. Lambiase F (2015) Joinability of different thermoplastic polymers with aluminium AA6082 sheets by mechanical clinching. Int J Adv Manuf Technol 80(9–12):1995–2006
2. He X, Gu F, Ball A (2014) A review of numerical analysis of friction stir welding. Prog Mater Sci 65:1–66
3. Lambiase F, Durante M, Di Ilio A (2016) Fast joining of aluminum sheets with Glass Fiber Reinforced Polymer (GFRP) by mechanical clinching. J Mater Process Technol 236:241–251
4. Vorderbrueggen J, Meschut G (2019) Investigations on a material-specific joining technology for CFRP hybrid joints along the automotive process chain. Compos Struct 230:111533
5. Pramanik A, Basak AK, Dong Y, Sarker PK, Uddin MS, Littlefair G, Dixit AR, Chattopadhyaya S (2017) Joining of carbon fibre reinforced polymer (CFRP) composites and aluminium alloys-a review. Compos Part A 101:1–29
6. Lambiase F, Ko DC (2017) Two-steps clinching of aluminum and Carbon Fiber Reinforced Polymer sheets. Compos Struct 164:180–188
7. Liu Y, Zhuang W, Shi H (2019) Influencing factors on fatigue performance of self-piercing riveted joints: a review. Mater Rep 33(11):1825–1830 in Chinese
8. Xing B, He X, Wang Y, Yang H, Deng C (2014) Study of mechanical properties for copper alloy H62 sheets joined by self-piercing riveting and clinching. J Mater Process Technol 216:28–36
9. Lei L, He X, Yu T, Xing B (2019) Failure modes of mechanical clinching in metal sheet materials. Thin-Walled Struct 144:106281
10. Zhang Y, He X, Zeng K, Lei L, Gu F, Ball A (2017) Influence of heat treatment on mechanical properties of clinched joints in titanium alloy sheets. Int J Adv Manuf Technol 91(9–12):1–13
11. Tenorio MB, Lajarin SF, Gipiela ML, Marcondes PVP (2019) The influence of tool geometry and process parameters on joined sheets by clinching. J Braz Soc Mech Sci Eng 41:67–78
12. Xing B, He X, Zeng K, Wang Y (2014) Mechanical properties of self-piercing riveted joints in aluminum alloy 5052. Int J Adv Manuf Technol 75(1–4):351–361
13. Liu Y, Zhuang W (2019) Self-piercing riveted-bonded hybrid joining of carbon fibre reinforced polymers and aluminium alloy sheets. Thin-Walled Struct 144:106340
14. Liang J, Jiang H, Zhang J, Wu X, Zhang X, Li G, Cui J (2019) Investigations on mechanical properties and microtopography of electromagnetic self-piercing riveted joints with carbon fiber reinforced plastics/aluminum alloy 5052. Arch Civ Mech Eng 19:240–250
15. Rao HM, Kang J, Huff G, Avery K (2018) Impact of specimen configuration on fatigue properties of self-piercing riveted aluminum to carbon fiber reinforced polymer composite. Int J Fatigue 113:11–22
16. Qin G, Na J, Mu W, Tan W, Yang J, Ren J (2018) Effect of continuous high temperature exposure on the adhesive strength of epoxy adhesive, CFRP and adhesively bonded CFRP-aluminum alloy joints. Compos Part B Eng 154:43–55
17. Lambiase F, Paoletti A, Grossi V, Di Ilio A (2019) Analysis of loads, temperatures and welds morphology in FSW of polycarbonate. J Mater Process Technol 266:639–650
18. Lambiase F, Paoletti A, Di Ilio A (2016) Friction spot stir welding of polymers: control of plunging force. Int J Adv Manuf Technol 90(9–12):2827–2837
19. Eslami S, De Figueiredo MAV, Tavares PJ, Moreira PMGP (2017) Parameter optimisation of friction stir welded dissimilar polymers joints. Int J Adv Manuf Technol 94(5–8):1759–1770
20. He X (2017) Clinching for sheet materials. Sci Technol Adv Mater 18(1):381–405
21. Lee CJ, Lee SH, Lee JM, Kim BH, Kim BM, Ko DC (2014) Design of hole-clinching process for joining CFRP and aluminum alloy sheet. Int J Precis Eng Manuf 15:1151–1157
22. Lee SH, Lee CJ, Lee KH, Lee JM, Kim BM, Ko DC (2015) Influence of tool shape on hole clinching for carbon fiber-reinforced plastic and SPRC440. Adv Mech Eng 6:810864
23. Lee CJ, Kim BM, Kang BS, Song WJ, Ko DC (2017) Improvement of joinability in a hole clinching process with aluminum alloy and carbon fiber reinforced plastic using a spring die. Compos Struct 173:58–69
24. Lambiase F, Paoletti A (2018) Friction-assisted clinching of aluminum and CFRP sheets. J Manuf Process 31:812–822
25. Lee CA, Shen G, Kim BM, Lambiase F, Ko DC (2018) Analysis of failure-mode dependent joint strength in hole clinching from the aspects of geometrical interlocking parameters. Metals 8(12):1020

Publisher's note Springer Nature remains neutral with regard to jurisdictional claims in published maps and institutional affiliations.